

# Solar Probe Plus MAG Sensor Thermal Design for Low Heater Power and Extreme Thermal Environment

Michael K. Choi

*NASA Goddard Space Flight Center, Greenbelt, MD 20771*

The heater power available for the Solar Probe Plus FIELDS MAG sensor is less than half of the heritage value for other missions. Nominally the MAG sensors are in the spacecraft's umbra. In the worst hot case, approximately 200 spacecraft communication downlinks, up to 10 hours each, are required at 0.7 AU. These downlinks require the spacecraft to slew 45° about the Y-axis, exposing the MAG sensors and boom to sunlight. This paper presents the thermal design to meet the MAG sensor thermal requirements in the extreme thermal environment and with low heater power. A thermal balance test on the MAG sensor engineering model has verified the thermal design and correlated the thermal model for flight temperature predictions.

## Nomenclature

$\alpha$	=	solar absorptance
$AC$	=	alternating current
$AFT$	=	allowable flight temperature
$AU$	=	astronomical unit
$CTE$	=	coefficient of thermal expansion
$DC$	=	direct current
$CDR$	=	Critical Design Review
$Comm$	=	communication
$\varepsilon$	=	hemispherical emittance
$e^*$	=	effective emittance
$EM$	=	engineering model
$ESA$	=	European Space Agency
$GSE$	=	ground support equipment
$ISAS$	=	Institute of Space and Astronautical Science
$ITO$	=	indium tin oxide
$R_s$	=	solar radii
$MAG$	=	Magnetometer
$MLI$	=	multilayer insulation
$SiO_x$	=	silicon oxide
$SPP$	=	Solar Probe Plus
$TC$	=	thermocouple
$VDA$	=	vacuum deposited aluminum

## I. Introduction

**S**OLAR Probe Plus (SPP) is a NASA's Living with a Star mission. It is scheduled for launch from Cape Canaveral in July 2018. The primary scientific goal of the SPP mission is to understand how the Sun's corona is heated and how the solar wind is accelerated. A combination of in situ measurements and imaging will be used to achieve this goal. The spacecraft is three-axis stabilized. It uses guidance and control sensors and attitude control thrusters to maintain the thermal protection system primary sunshield pointing toward the Sun. Fig. 1 shows the spacecraft. Fig. 2 shows the baseline SPP trajectory. It uses Venus flybys to reach a minimum perihelion of 8.5 solar radii ( $R_s$ ) or about  $6 \times 10^6$  km of the Sun's "surface" in approximately 6.5 years.

The Magnetometer (MAG) is a unit of the SPP FIELDS instrument which will make direct measurements of electric and magnetic fields, radio emissions, and shock waves that course through the Sun's atmospheric plasma. It

includes two sensors, inboard unit and outboard unit, which are mounted to a deployable boom (Fig. 1 and Fig. 3), and two circuit cards which are part of the FIELDS electronics box mounted to a spacecraft equipment panel. The MAG is provided by NASA's Goddard Space Flight Center (GSFC). This paper is in conjunction with the MAG sensors.

The two MAG sensors are separated by a distance of 0.8 m. The inboard sensor is approximately 1.9 m from the spacecraft aft end. The MAG boom is made of M55J composite that has a very low coefficient of thermal expansion (CTE), and is hollow. There is a connector plate about half way between the MAG sensors. Each MAG sensor has a pigtail harness that connects it to the connector plate. A spacecraft-provided harness connects the connector plate to the FIELDS electronics box.

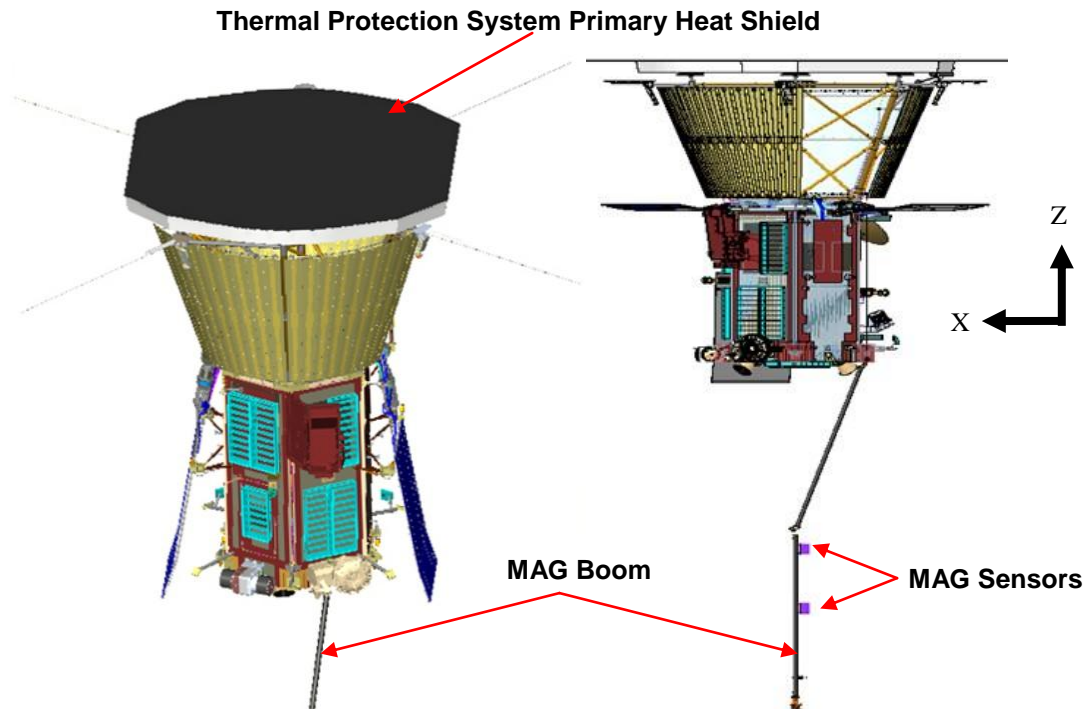


Figure 1. SPP with Solar Array Panels Stowed (Left) and Deployed (Right) (credit: JHU APL and NASA).

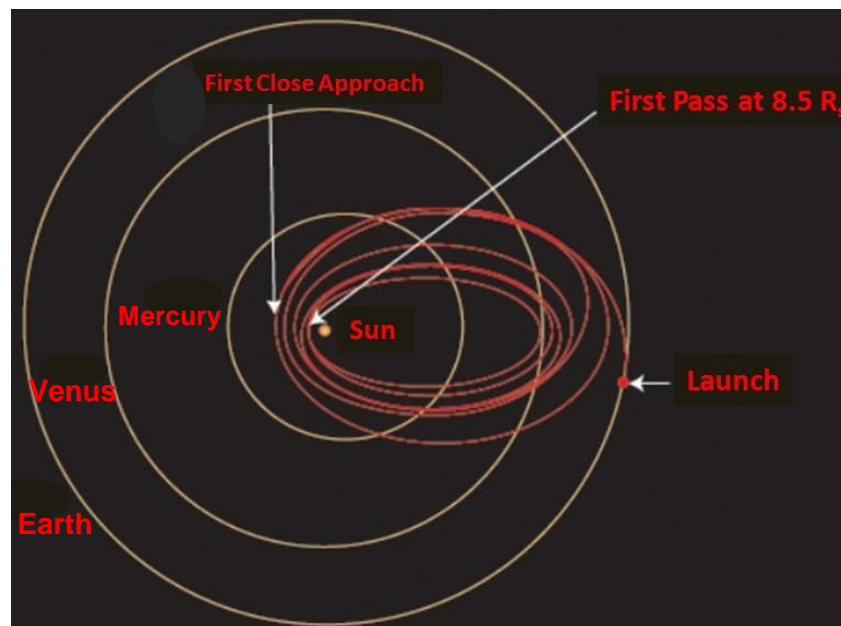


Figure 2. SPP Trajectory (credit: JHU APL and NASA).

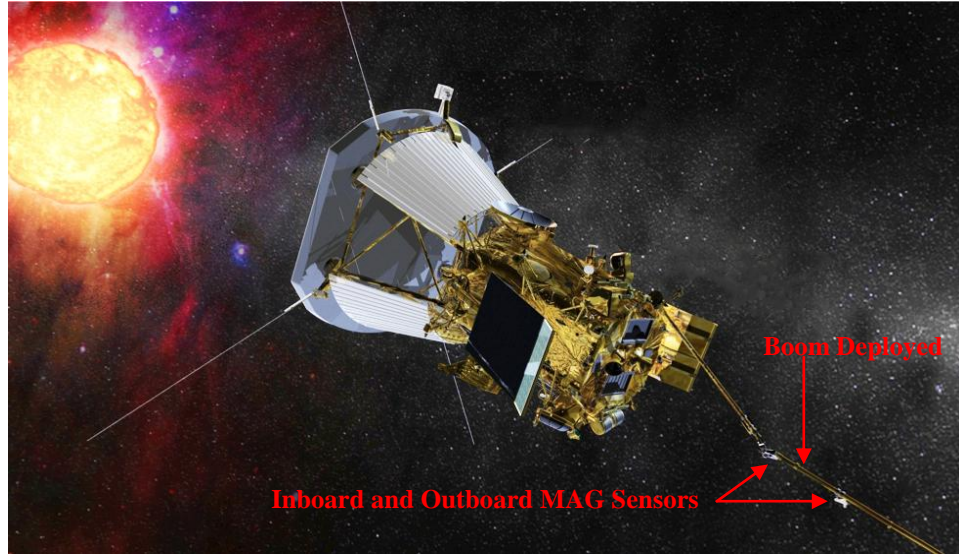


Figure 3. Location of MAG Sensors (credit: JHU APL and NASA).

## II. SPP MAG Sensor Thermal Characteristics

For a MAG sensor that measures weak interplanetary fields, the in-flight determination of zero levels is a crucial step of the overall calibration procedure<sup>1</sup>. Post-launch spacecraft MAG sensor zero levels can differ from their pre-launch values for many reasons. One of the most common issues is temperature changes of the sensor. A general review on space-based MAGs presented by Mario Acuna<sup>2</sup> also discussed this. To maintain the fluxgate MAG sensors within their optimum operating temperature range, it is necessary to provide heater power to the sensor assemblies<sup>3</sup>.

Since it is extremely difficult to reduce the stray magnetic field associated with the operation of DC powered heater to acceptable levels for the MAG sensor, a magnetic amplifier operating at 50 kHz is used to obtain automatic, proportional control of AC power supplied to the heating elements<sup>3</sup>. The proportional heater controller temperature range of  $-15^{\circ}\text{C}$  to  $23^{\circ}\text{C}$  used for the Juno MAG sensor is a reasonable choice for the SPP MAG sensors. A temperature range like  $-15^{\circ}\text{C}$  to  $23^{\circ}\text{C}$  allows the MAG sensor heater to function as temperatures vary in the operating range without turning on and off abruptly. The approximately  $40^{\circ}\text{C}$  range also allows for possible in-flight deviations from predicted temperatures.

The GSFC fluxgate MAG sensor is a high-heritage instrument. It has been or being flown on numerous NASA, ESA and ISAS missions, such as Voyager, AMPTE, MAGSAT, Giotto, DMSp, WIND, CLUSTER, MGS, GEOTAIL, Lunar Prospector, MESSENGER, STEREO, Juno and MAVEN. The MAG sensor is calibrated in the laboratory. Its minimum operating allowable flight temperature limit (AFT) is  $-20^{\circ}\text{C}$ . It is a heritage value from those missions. It is to optimize the MAG performance capabilities by ensuring in-flight calibration stays at nominal value<sup>4</sup>. The MESSENGER MAG sensor, for example, is maintained at no colder than  $-15^{\circ}\text{C}$  by heater during normal operations<sup>5</sup>. The Juno MAG sensor is also maintained at no colder than  $-15^{\circ}\text{C}$  by heater during normal operations. The maximum operating AFT limit is  $40^{\circ}\text{C}$ . It is also to optimize the MAG performance. The maximum non-operating AFT limit is  $60^{\circ}\text{C}$ . Table 1 is a summary of the AFT limits.

Table 1. AFT Limits ( $^{\circ}\text{C}$ ).

Operating		Non-Operating	
Minimum	Maximum	Minimum	Maximum
-20	40	-40	60

Fig. 4 shows the SPP FIELDS MAG sensor engineering model (EM). Its enclosure consists of a base plate and a cover; both are made of carbon composite which has low thermal conductivity, low CTE and high emittance. The sensor size is 12.471 cm x 7.62 cm x 7.62 cm. Two bobbins, one horizontal and one vertical, are attached to the carbon composite. A heater, which consists of strips, is attached to the carbon composite underneath the bobbins.

There is no contact between the heater and bobbins. The MAG sensor pigtail harness is 0.3556 m (14 inch) long. Two heater controller thermistors are attached to a phenolic strip which has heat radiation exchange with its surrounding.

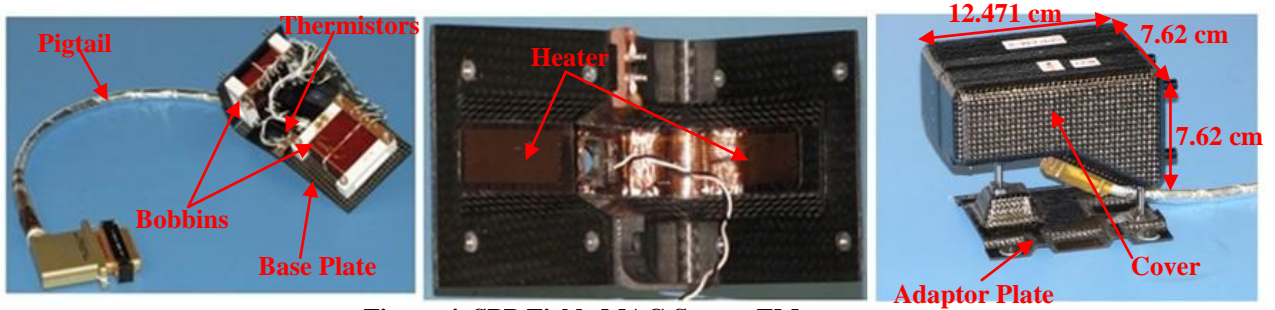


Figure 4. SPP Fields MAG Sensor EM.

### III. SPP Mission Extreme Thermal Environment for MAG Sensors

The power dissipation of each MAG sensor is only 0.05 W or less. It is an order of magnitude smaller than the heat leak of the sensor. The thermal environment drives the temperatures of the MAG sensor. Since the same heater and heater controller set-point are used for both the operating and non-operating (survival) modes, in the same cold case thermal environment the temperature difference between operating and non-operating is less than 5°C. The worst hot case and worst cold case extreme thermal environment of the SPP mission for the MAG sensors is as follows.

#### A. Worst Hot Non-operating Case

The Comm Slew (Downlink) at 0.7 AU is the worst hot case for the SPP MAG sensors. The solar irradiance is  $2790 \text{ Wm}^{-2}$  (2.04 suns). The spacecraft slews 45° about the Y-axis for approximately 200 times for downlinks (Fig. 5). Each Downlink is up to 10 hours. The MAG is non-operating in this case. During each Downlink, the MAG sensors and boom are exposed to the sun. Due to solar exposure, the MAG sensor temperature will increase. When the spacecraft slews back to its nominal attitude, the MAG sensors and boom are in the umbra, and will cool down. The temperature cycling of the MAG sensors will repeat for approximately 200 times.

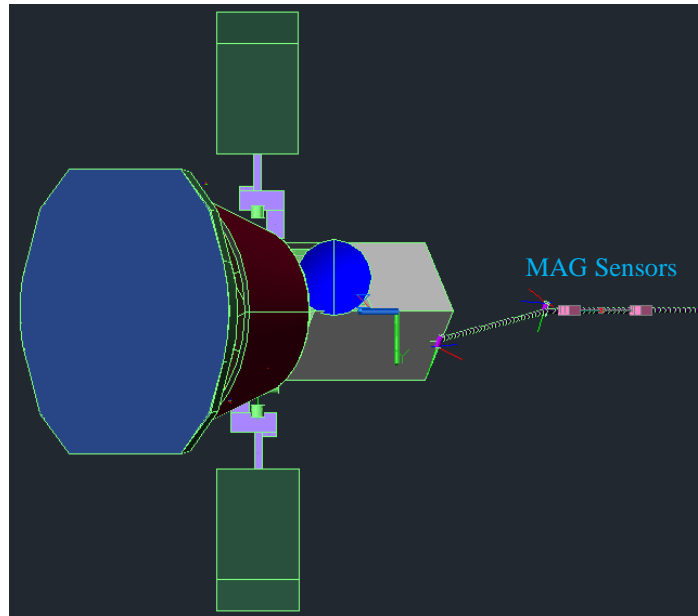
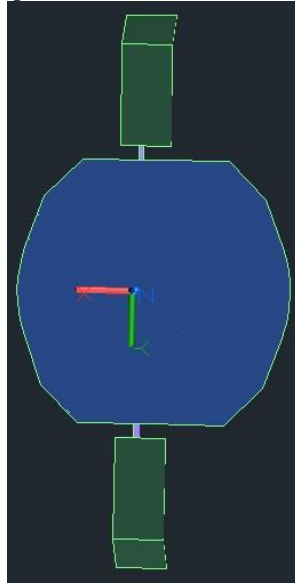


Figure 5. View from Sun during Comm Slew (Downlink) at 0.7 AU.

### B. Worst Cold Operating Case

The spacecraft is at its nominal attitude during instrument checkout, cruise, fanbeam and solid state recorder playbacks at 0.82 AU (Fig. 6). Instruments are powered on. The MAG sensors are in the spacecraft's umbra.



**Figure 6. View from Sun during Instrument Operation at 0.82 AU.**

### C. Worst Cold Non-operating Case

The Comm Slew (Downlink) at 0.76 to 0.28 AU is the worst cold non-operating case. The spacecraft does not slew for approximately 700 Downlinks (Fig. 7). Each Downlink is up to 10 hours. Instruments are powered off. The MAG sensors are in the spacecraft's umbra.

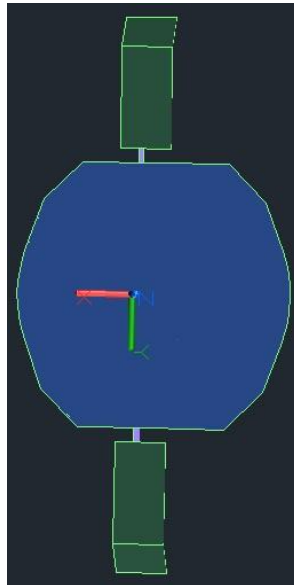


**Figure 7. View from Sun during Downlink at 0.76 to 0.26 AU.**

## IV. SPP Heater Power Budget for MAG Sensors

The SPP heater power budget for the MAG sensors is limited. The allocation at the FIELDS instrument Critical Design Review (CDR) is 1.86 W orbital average per sensor. Only 1.3 W (or 70%) goes to the heater because 0.56 W (or 30%) is consumed by the heater controller which is within the MAG circuit cards. The heater power is much smaller than the flight heritage value.



## V. Objective

The objective of this paper is to present the thermal design of the SPP FIELDS MAG sensors to meet the thermal requirement with extreme thermal environment and low heater power budget.

## VI. SPP FIELDS MAG Sensor Thermal Design and Analysis

In the worst cold case thermal environment, the SPP FIELDS MAG sensors lose heat by a) radiation to cold space, b) conduction through the mounts to the boom, and c) conduction through the pigtail harness which radiates heat to space and conducts heat to the connector plate. As a flight heritage thermal design, the MAG sensor enclosure and pigtail harness are insulated with multi-layer insulation (MLI) blankets. The sensor base plate is thermally isolated from the boom mounting interface. A boom interface Ti-6Al-4V bracket has been designed by the SPP spacecraft contractor. It wraps around the boom tube. Fig. 8 illustrates the heat leak paths from the MAG sensor by conduction and radiation.

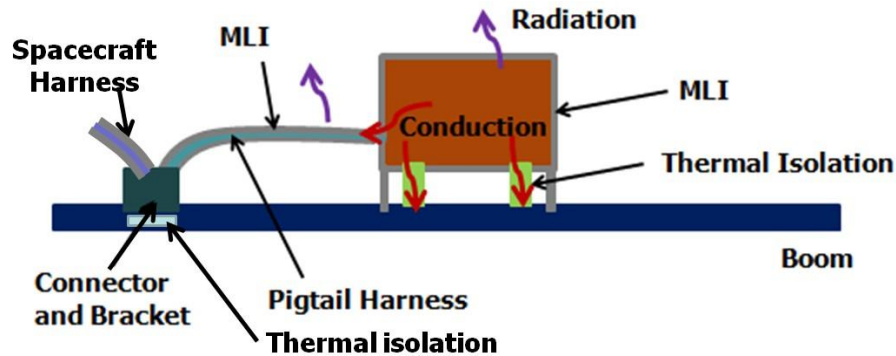


Figure 8. SPP FIELDS MAG Sensor Heat Leak Paths.

### A. Issue with Heritage Thermal Design for SPP MAG

The results of the MAVEN MAG sensor cold thermal balance test at GSFC provided an implication for the thermal issue of low heater power for the SPP MAG sensors if the heritage thermal design is used. With a 2.2 W heater power, a  $-50^{\circ}\text{C}$  mounting interface temperature and a liquid nitrogen cooled chamber shroud, the steady state sensor temperature was  $-22^{\circ}\text{C}$  in the test. If same thermal design is used for SPP MAG sensors, with 1.3 W heater power the sensor temperature will be much colder than the heritage minimum limit of  $-20^{\circ}\text{C}$ . The low heater power allocation drives changes to the heritage thermal design for the SPP MAG sensors.

### B. Thermal Design Changes

To reduce heat leak by conduction, the following design changes have been made:

- Neptape 1526 replaces copper over-braid for magnetic shielding of pigtail harness.
- Kinematic mounts (3) replace G-10 standoffs (4) and fasteners (4) used on MAVEN and other missions.
- 26 AWG, instead of 24 AWG, twisted pair shielded wires are used for heaters.
- 0.635 cm thick G-10 spacers thermally isolate sensor adaptor plate from boom mounting interface.
- 0.3175 cm thick G-10 washers thermally isolate fastener heads from boom mounting interface.

The kinematic mounts consist of six 0.1524 cm diameter Ti-6Al-4V screws and six equivalent point-contacts with 0.635 cm diameter silicon nitride (SiN) spheres. They thermally isolate the sensor base plate from the adaptor plate (Fig. 9). They have Juno MAG flight heritage, but are not identical (e.g., screws are longer and smaller in diameter).

The MAG sensor thermal (and mechanical) interface with the spacecraft is at the boom Ti-6Al-4V bracket and not at the boom tube. The thermal interface temperature only applies to the four mounting points of the boom Ti-6Al-4V bracket for the MAG sensor (Fig. 10). On the spacecraft side of the interface, thermal isolation between the boom Ti-6Al-4V bracket and boom tube is recommended to the spacecraft contractor to reduce heat conduction from the sensor to the boom tube. An option of thermal isolation is to minimize the contact area between the boom bracket and boom tube, and to add low emittance (e.g., aluminized Kapton tape) to the boom bracket interior and boom tube exterior underneath the boom bracket.

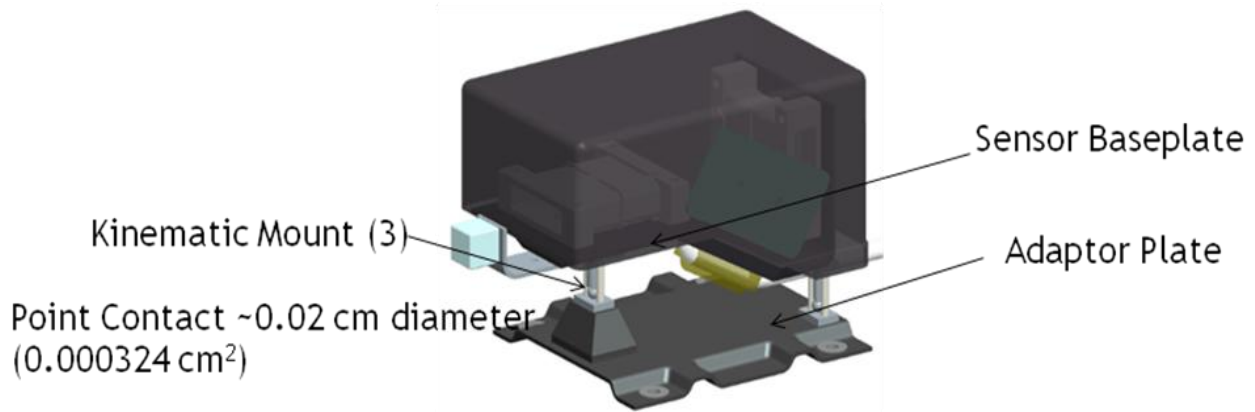


**Figure 9. Kinematic Mounts.**

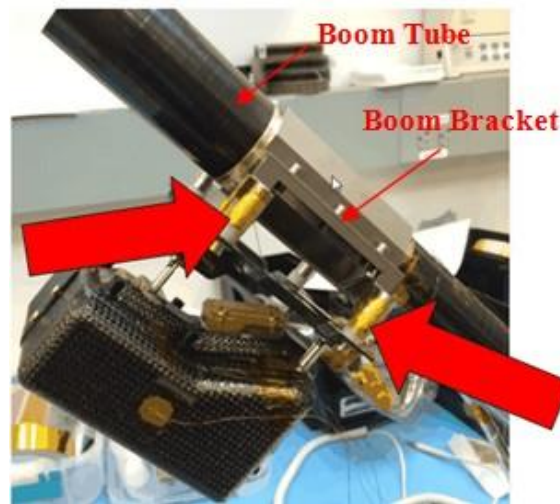


**Figure 10. Thermal and Mechanical Interface (4 Places) in EM Thermal Balance Test.**

To reduce heat leak by radiation, the following design changes have been made. Due to the low heater power budget, a key thermal design parameter for the SPP MAG sensors is the MLI effective emittance ( $\epsilon^*$ ). To minimize the thermal effect of 3K space in the worst cold case and solar flux at 0.7 AU (Downlink) in the worst hot case, 40 layers of MLI (a 15-layer MLI blanket on top of a 25-layer MLI blanket to allow flexibility) for the MAG sensor are used. Also 35 layers of MLI (a 15-layer MLI blanket on top of a 20-layer MLI blanket to allow flexibility) for the MAG pigtail are used. Note that a 20-layer or 25-layer MLI blanket on MAG sensors has high flight heritage. Therefore each individual MLI blanket in the EM thermal balance test had flight heritage number of layers, despite that the total number of layers of the two MLI blankets is larger than heritage.

On the spacecraft side, the boom tube and boom Ti-6Al-4V brackets are also insulated with MLI blankets. The boom MLI is attached to the MAG sensor MLI in the vicinity of the adaptor plate (Fig. 11).

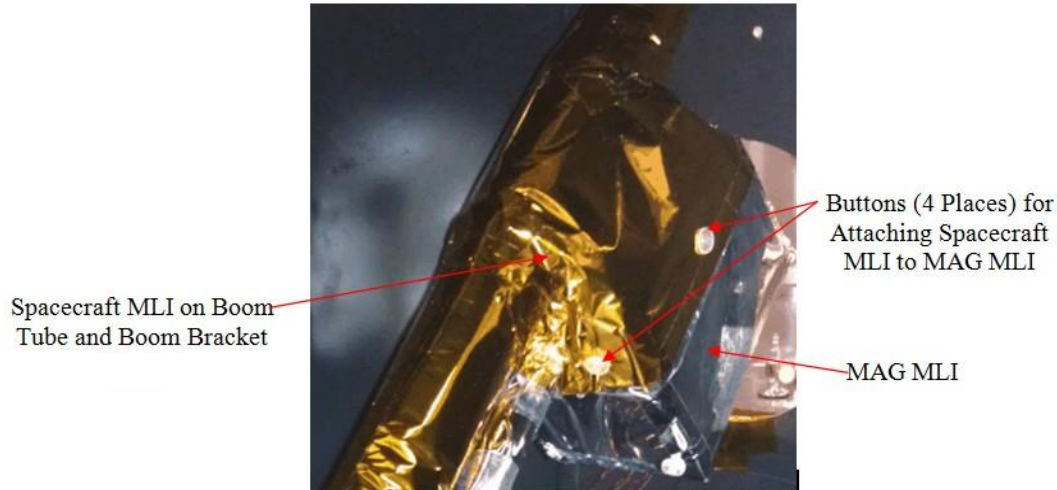


**Figure 11. MLI Interface in EM Thermal Balance Test.**

### C. Thermal Analysis

The total thermal conductance from the sensor base plate to the adaptor plate was estimated to be  $0.0104 \text{ W}^\circ\text{C}^{-1}$ , which includes  $0.006 \text{ W}^\circ\text{C}^{-1}$  for six equivalent point-contacts and  $0.00444 \text{ W}^\circ\text{C}^{-1}$  for six Ti-6AL-4V screws.<sup>6</sup> The total thermal conductance between the sensor adaptor plate and boom bracket was estimated to be  $0.02 \text{ W}^\circ\text{C}^{-1}$ . The sensor enclosure and adaptor plate MLI  $\epsilon^*$  was assumed to be 0.05, since the MLI is very small. The lengths of the outboard and inboard pigtail harness are assumed to be 0.3556 m long. Each harness has 16 nodes for conductors and 32 nodes for MLI blankets. The conductors include 16 copper wires (26 AWG) and Neptape aluminum (2 layers 0.00889 mm each). The conductor's node-to-node thermal conductances are  $0.041 \text{ W}^\circ\text{C}^{-1}$ . The harness MLI  $\epsilon^*$  was assumed to be 0.1 by using a tubular MLI design.

On the spacecraft side, with thermal isolation, a  $0.16 \text{ W}^\circ\text{C}^{-1}$  conductance between the boom tube and boom bracket was assumed. The boom tube and boom bracket are assumed to be insulated with MLI blankets that have an  $\epsilon^*$  of 0.05 because they are very small in size. An Ultem spacer between the pigtail and boom tube was assumed. The connector bracket is assumed to be conductively isolated from the boom by Ultem standoffs and radiatively isolated from space by MLI.

The boom is a hollow M55J tube with a 3.8 cm diameter and 1.5 mm thick wall. Heat conduction along the boom's longitudinal (Z) axis is negligible (Fig. 12 and Fig. 13). However, its interior is black and has a high emittance and is non-specular. The boom segment under the boom bracket has no view to space. The interior of this segment can only radiate heat to the interior of the other boom segments. As the distance from the mounting interface increases, the view factor from the boom segment under the boom bracket to other boom segments decreases. Since the boom interior is non-specular, the heat radiation from the boom segment under the boom bracket to other boom segments decreases as the distance from the mounting interface increases (Fig. 12 and Fig. 13). In the worst cold case, the majority of the heat leaked to the spacecraft mounting interface from the MAG sensor is radiated to space through the MLI over the boom bracket and boom segments adjacent to the mounting interface. A minority of it is radiated to space through the MLI over the other boom segments.

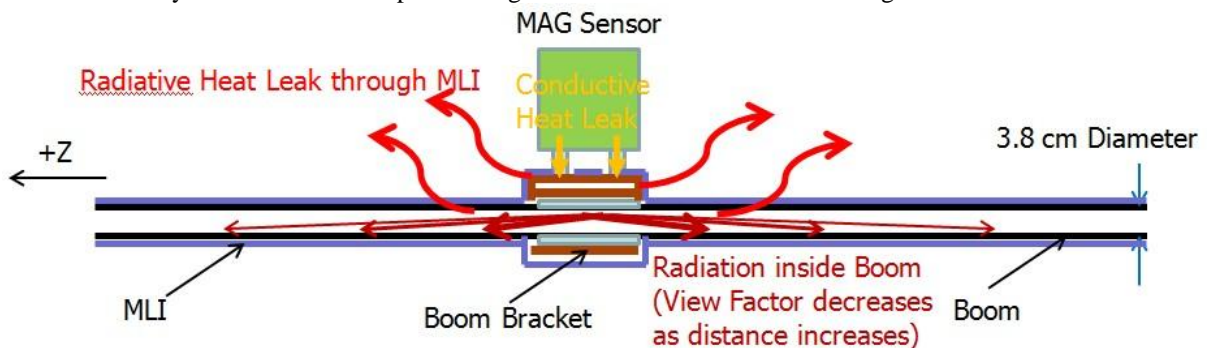


**Figure 12. Heat Leak from MAG Sensor to Boom.**



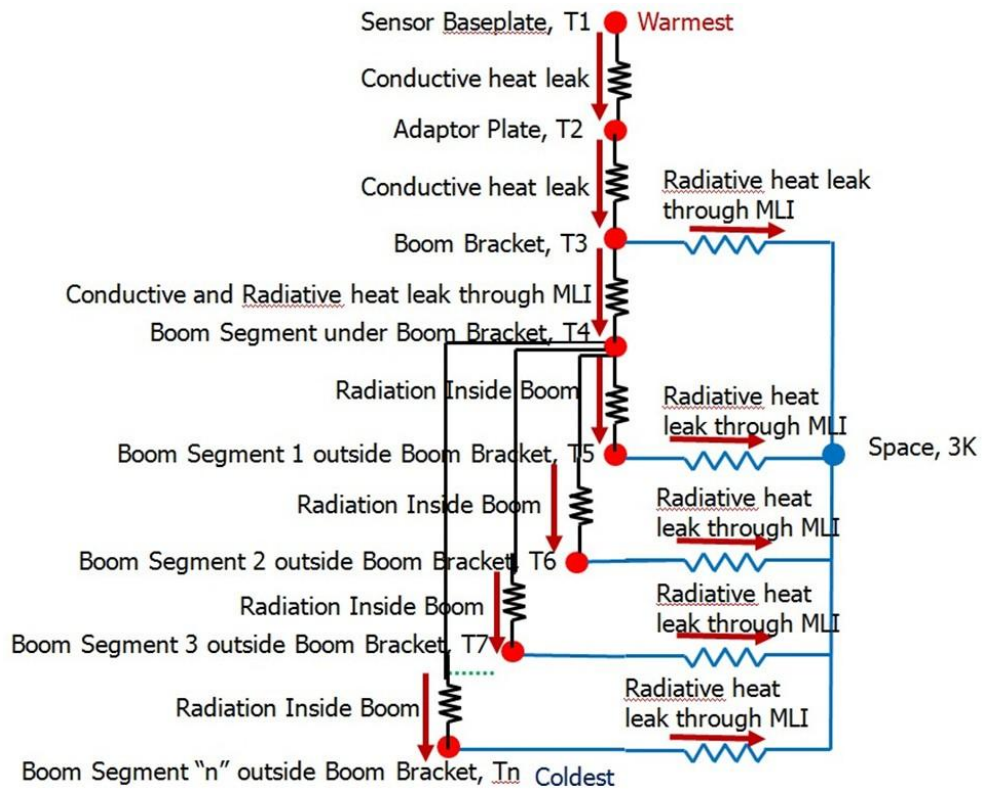


**Figure 13. Thermal Resistance Network.**

Fig. 14 and Fig. 15 show the SPP MAG sensor and boom integrated thermal model. The thermal nodes are as follows:

- 90 nodes for each sensor.
- 10 nodes for each boom bracket.
- 2 nodes for the connector bracket.
- 64 nodes for the outboard boom.
- 64 nodes for the inboard boom.
- 96 nodes for the spacecraft harness from the connector bracket to the Fields electronics box.
- 24 nodes (boundary temperatures) for the spacecraft.

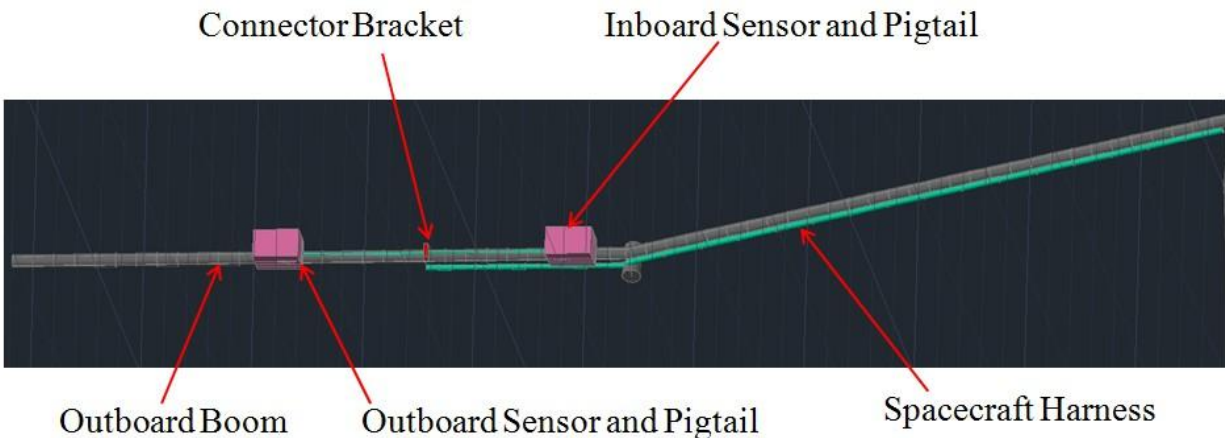


**Figure 14. MAG Sensor and Boom Integrated Thermal Model.**



**Figure 15. Thermal Model in Worst Hot Case.**

StaMet black Kapton is used as the outer cover of all spacecraft MLI blankets. The worst hot case thermal analysis results show that if this coating is used for the MAG, the MLI outer cover is very hot ( $>133^{\circ}\text{C}$ ) in the Comm Slew Downlink mission phase. A high temperature MLI layup with embossed Kapton as inner layers is needed. Testing at Jet Propulsion Laboratory showed that the  $e^*$  of this type of MLI is 19% larger than that with Dacron or Polyester netting spacers<sup>7</sup>. Also it would require a high temperature bakeout at  $143^{\circ}\text{C}$  or warmer. Therefore StaMet black Kapton is not used for the MAG sensor MLI outer cover. Instead, the GSFC flight heritage ITO/SiOx/VDA/Kapton coating, which has a much lower ratio of absorptance to hemispherical emittance (0.42 versus 0.75 at EOL; Table 2), is used. It reduces the MLI outer cover temperature by nearly  $60^{\circ}\text{C}$  in the worst hot case. Note that the BOL optical properties of ITO/SiOx/VDA/Kapton were recently measured at GSFC. The worst hot case maximum temperature prediction of ITO/SiOx/VDA/Kapton meets Dacron netting maximum temperature limits, intermittent or continuous, with adequate margin. Also ITO/SiOx/VDA/Kapton is electrically conductive, and meets the  $10^5 \Omega$  per square mission requirement.

To prevent the ITO/SiOx coating from damaged by folding or sharp bending radii, ITO/SiOx/VDA/Kapton is attached to the aluminized Kapton MLI outer cover by transfer adhesive after the MLI is installed.

**Table 2. Comparison of Absorptance and Emittance between StaMet and ITO/SiOx/VDA/Kapton.**

	Cold Case		Hot Case	
	BOL $\alpha$	BOL $\varepsilon$	EOL $\alpha$	EOL $\varepsilon$
StaMet black Kapton	0.49	0.84	0.56	0.75
ITO/SiOx/VDA/Kapton	0.13	0.52	0.20	0.48

Fig. 16 presents worst cold case sink temperatures at 0.82 AU. Fig. 17 presents worst hot case sink temperatures at 0.7 AU during the Comm Slew Downlink.

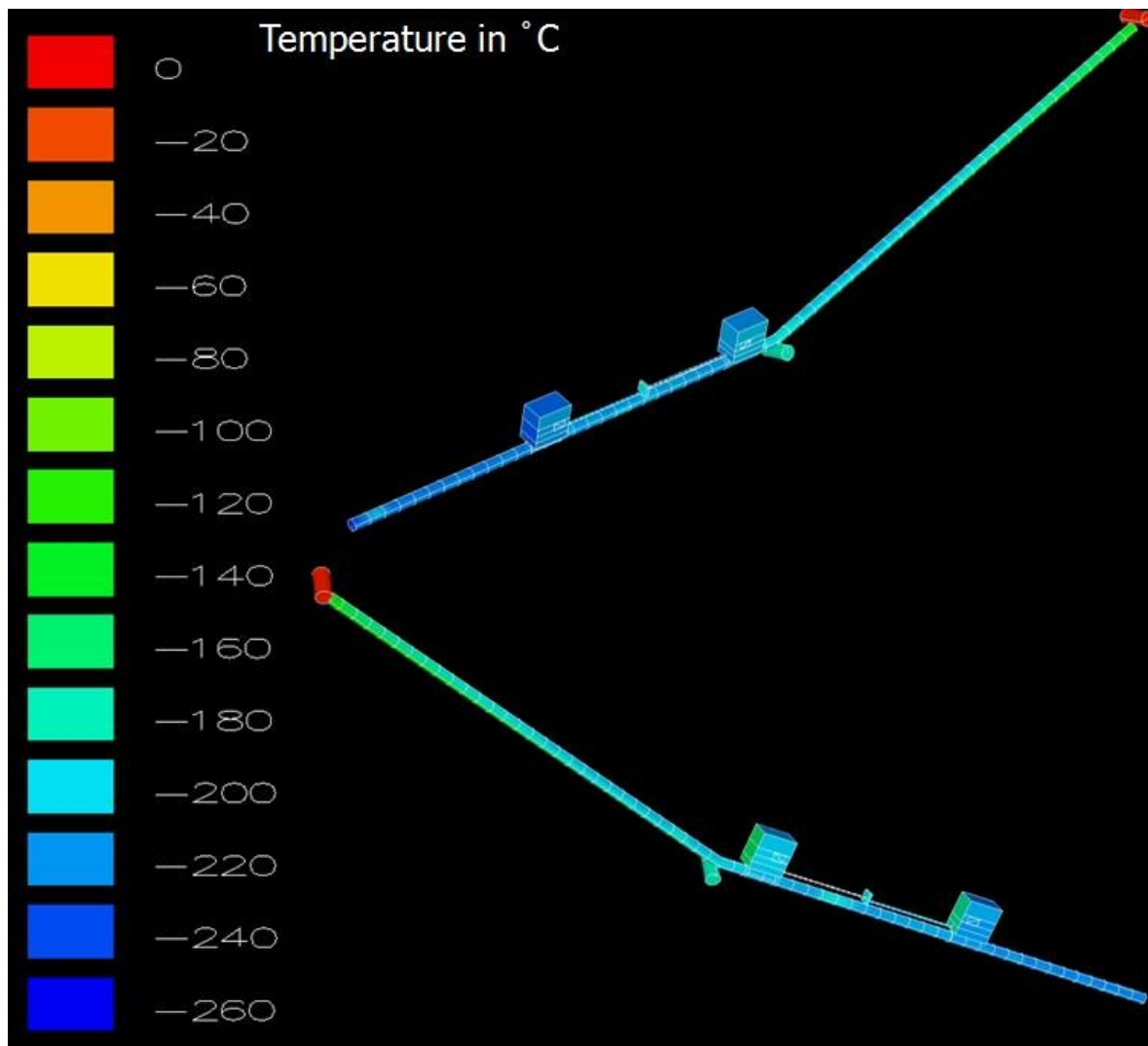
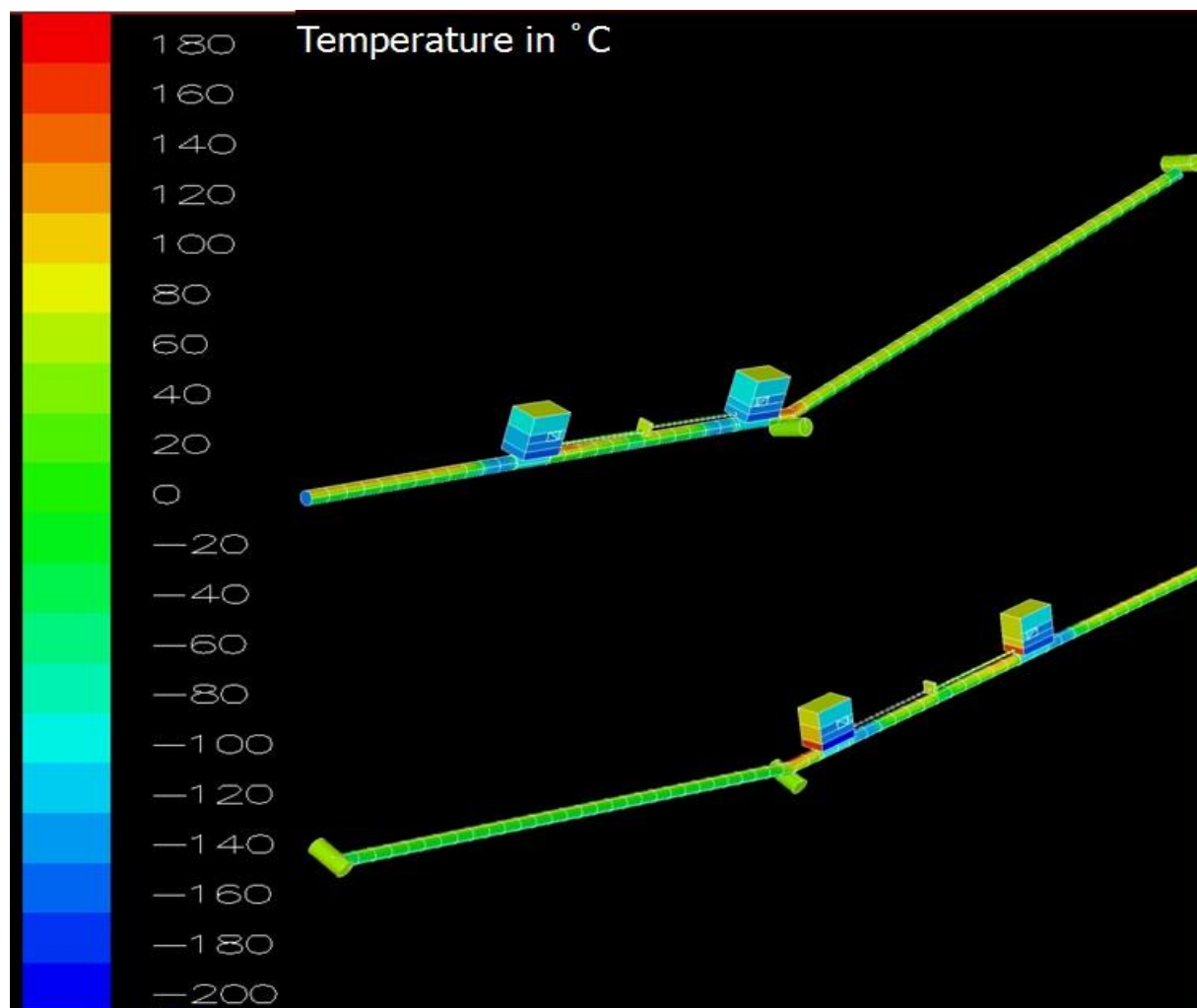


Figure 16. Worst Cold Case Sink Temperature Predictions.



**Figure 17. Worst Hot Case Sink Temperature Predictions.**

StaMet (boom MLI coating) and Germanium black Kapton (GBK) basically have the same optical properties. GSFC measured the specularity of GBK to be 0.69. The specularity of StaMet should be the same. The solar absorptance of ITO/SiOx/VDA/Kapton is significantly lower than that of StaMet (0.42 versus 0.75). Therefore if sunlight is incident on the MAG sensor MLI (in the Downlink worst hot case at 0.7 AU), 80% of it is reflected to the boom. Also the specularity of ITO/SiOx/VDA/Kapton is higher than that of StaMet (0.9 versus 0.69). The specular reflection of sunlight from the MAG sensor MLI blanket to the boom is 90% of the reflection. Also there is sunlight reflected between the boom bracket MLI and boom tube MLI.

The MAG sensor thermal effort has emphasized on the sensor, boom bracket and boom tube integrated thermal analysis by using the optical properties of ITO/SiOx/VDA/Kapton for the MAG sensor MLI and StaMet for the boom MLI. The results of the integrated thermal analysis show that in the worst hot case (Downlink at 0.7 AU), due to highly specular reflection of sunlight between the MAG sensor MLI blanket and boom MLI blanket, and between the boom bracket MLI blanket and boom MLI blanket, the maximum temperature prediction of the boom MLI blanket is close to 180°C (Fig. 17). Also the results of integrated thermal analysis show that the temperature prediction of the boom MLI blanket that is shaded from the sun by the MAG sensor (Fig. 17) is -160°C or colder. The optical properties of the coating on the exterior MLI outer cover over the boom bracket and boom segments adjacent to the boom bracket have a large impact on the boom bracket temperature. A coating, such as ITO/SiOx, that has a lower ratio of absorptance to emittance, for these surfaces will reduce the MLI outer cover (or exposed M55J) temperature and was recommended to the spacecraft contractor. This will also assure even if the MLI is shorted, it won't cause overheating on the boom bracket.

The results of worst cold case thermal analysis showed that with 1.3 W heater power per sensor, the temperature prediction of the sensor is above the minimum operating AFT limit of -20°C or the minimum non-operating AFT

limit of  $-40^{\circ}\text{C}$ . The results of worst hot case thermal analysis showed that the sensor temperature prediction is about  $40^{\circ}\text{C}$  below the maximum non-operating AFT limit of  $60^{\circ}\text{C}$ .

## VII. Verification of SPP Fields MAG Sensor Thermal Design

Generally a thermal balance test for an instrument or spacecraft cannot be performed until the flight hardware (or at least an EM for an instrument) is built after the CDR. Without a correlated thermal model (i.e., model correlated to thermal balance test results), a common practice is to use a range of MLI  $\epsilon^*$  to bias the flight hardware colder in the worst cold case and warmer in the worst hot case.

A main goal of the EM MAG sensor thermal balance test before the CDR was to verify that 1.3 W heater power per MAG sensor achieves a sensor operating temperature within the heritage temperature range (no colder than  $-20^{\circ}\text{C}$  and preferably  $0^{\circ}\text{C}$ ). The test was performed in the Electrostatic Vacuum Chamber, which is a small vacuum chamber with a usable volume of 0.5 m diameter x 0.6 m height, located in the Solar Wind Facility at GSFC.

### A. Test Setup

In flight, the inboard and outboard MAG sensors are 0.8 m apart on the outboard boom (Fig. 18), and the connector bracket is approximately half way between them. The heat conduction paths from the sensors to the boom are also shown in Fig. 18. Only one EM MAG sensor was available for the thermal balance test. For the thermal balance test to be conservative, a 0.406 m long M55J carbon composite tube was used as the boom simulator (Fig. 19). Its diameter and wall thickness are the same as in flight. Also a boom Ti-6Al-4V bracket simulator was used. It was clamped to the boom tube simulator at a location to simulate the heat conduction paths from the sensor to the boom tube (Fig. 19). To reduce thermal contact between the boom Ti-6Al-4V bracket and boom tube simulators, 15-layers of Dacron netting were inserted at the interface between them. It was a quick, effective and no cost technique to separate the boom bracket from the boom tube. It also satisfied EM MAG mechanical mounting. Better and more effective techniques of thermal isolation are available for the flight hardware. An option was presented earlier.

At least two grounding straps are required for each thermal blanket to meet observatory-level electrostatic requirements. They were included in the thermal balance test to simulate heat leak by conduction.

The lower end of the boom tube simulator was thermally isolated from the test fixture by G-10 spacers. A connector plate simulator was thermally isolated from the test fixture. A GSE harness was used to supply voltage to the MAG sensor. It simulated the spacecraft harness between the connector plate and FIELDS electronics box in flight. The test fixture, connector bracket simulator and GSE harness were shielded from the chamber shroud wall by MLI.

A total of ten thermocouples were used. It is the maximum number that the vacuum chamber feedthrough can accommodate. Fig. 20 shows the locations of the thermocouples. Fig. 21 displays photographs of the test setup in the vacuum chamber prior to pumpdown. The chamber shroud was cooled by liquid nitrogen in the test. The chamber pressure was maintained at  $1 \times 10^{-6}$  torr or lower for the entire thermal balance test.

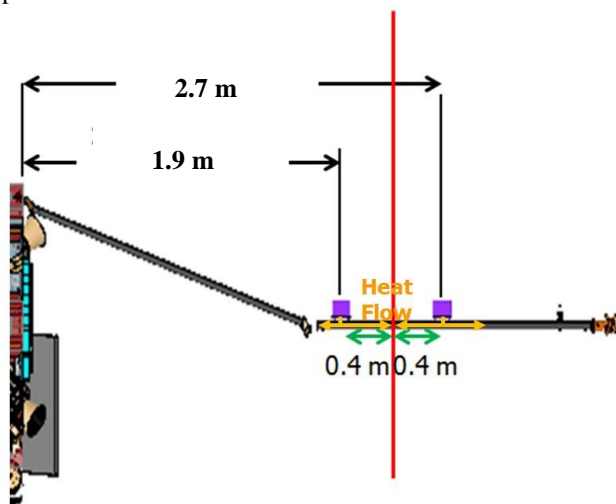


Figure 18. In-Flight MAG Sensors on Boom and Conduction Paths.

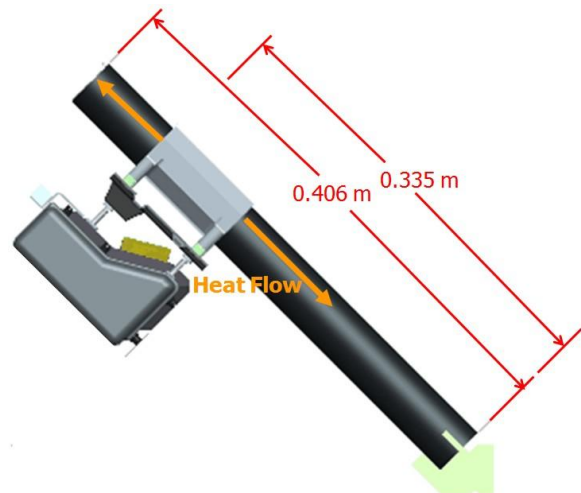
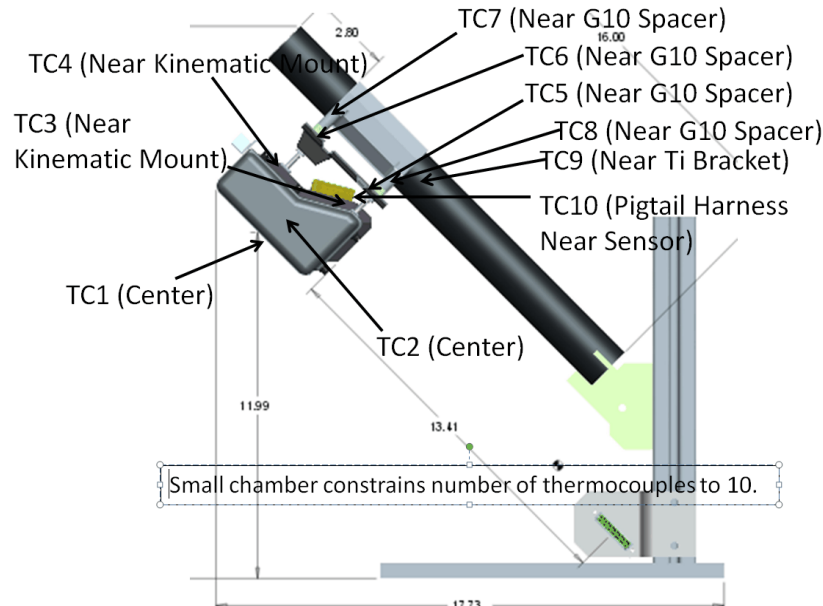
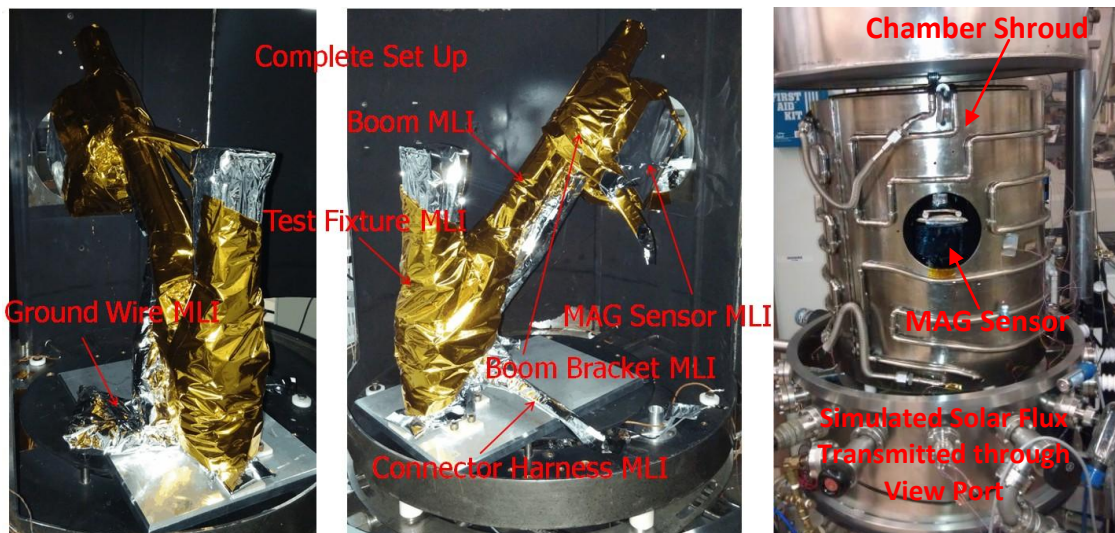


Figure 19. Boom Tube, Boom Bracket and Conduction Paths in Thermal Balance Test.





**Figure 20. Thermocouple Locations in Thermal Balance Test.**



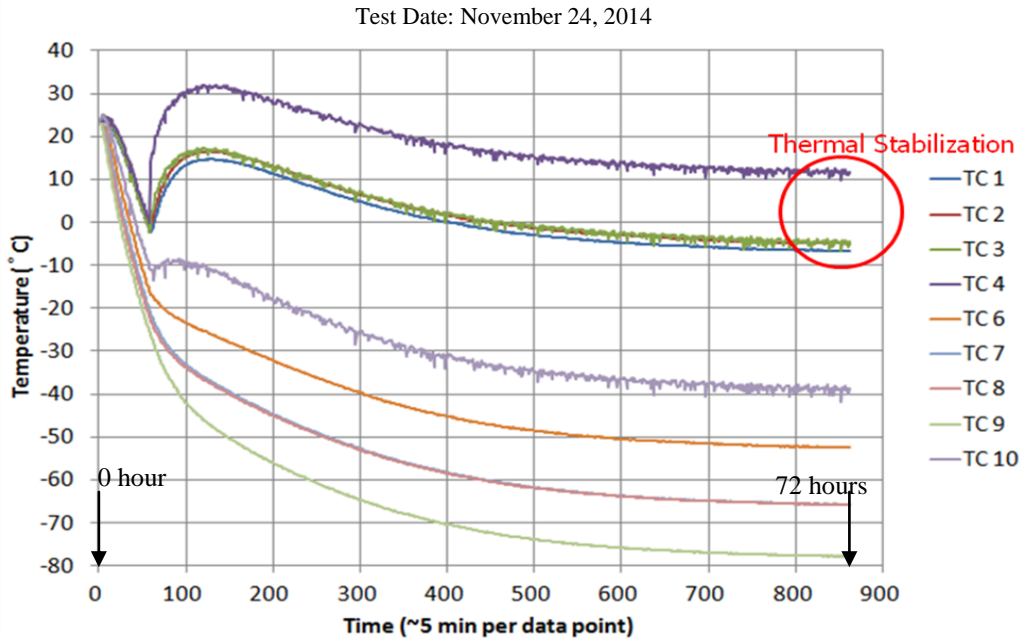
**Figure 21. Thermal Balance Test Setup before Pumpdown.**

### B. Thermal Balance Stabilization Criteria

Thermal balance stabilization occurs when the rates of change of the control thermocouples (TC1 and TC2) are  $0.1^{\circ}\text{C/hr}$  for two hours over a period of six consecutive hours, with a decreasing trend over the six-hour period.

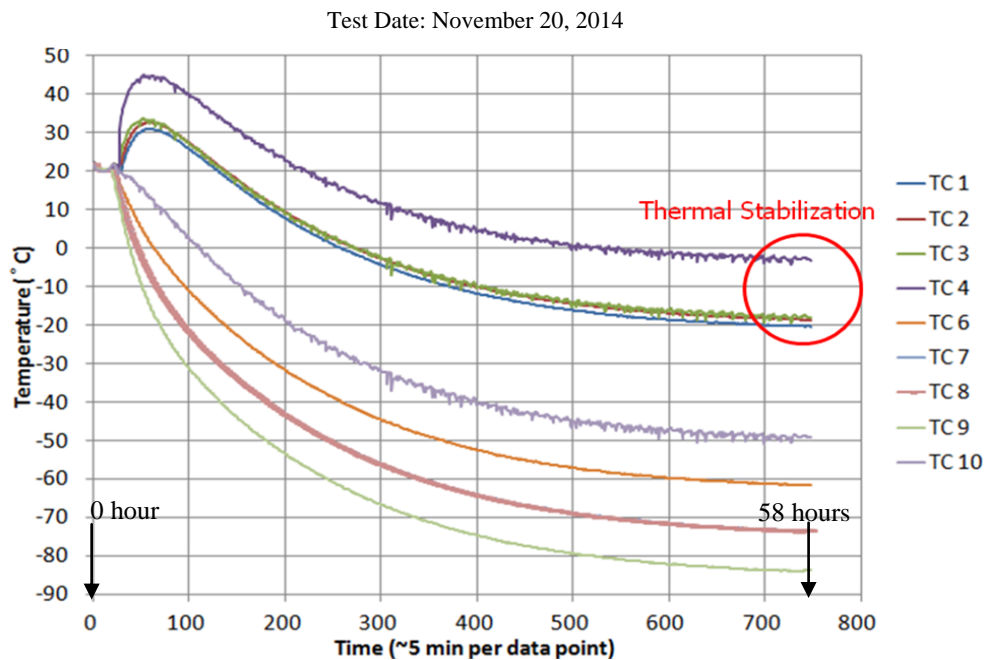
### C. Test Results

Fig. 22 presents the temperatures of the thermocouples in the cold non-operating thermal balance test with 1.3 W heater power for the EM MAG sensor. TC4, which was next to the heater, on the base plate was at  $11^{\circ}\text{C}$ . TC2 and TC3, which were on the cover, were at  $-4^{\circ}\text{C}$ . TC1, which was on the base plate and not next to the heater, was at  $-3^{\circ}\text{C}$ . From the thermal model, the temperatures of the bobbins are approximately the average ( $0^{\circ}\text{C}$ ) of TC1, TC2, TC3 and TC4. It agrees with the internal flight telemetry thermistor temperature. It meets the thermal requirement. The thermal balance test results show that 1.3 W is a reasonable heater power allocation. TC7 and TC8, which were on the spacecraft boom bracket side of the mounting interface, were at  $-65^{\circ}\text{C}$ . The boom tube temperature, which was adjacent to the boom bracket, was at  $-78^{\circ}\text{C}$ . The large temperature gradient ( $>70^{\circ}\text{C}$ ) between the sensor base plate and boom tube verifies adequate thermal isolation.



**Figure 22. Cold Case Non-Operating Thermal Balance Test Results for 1.3 W Heater Power.**

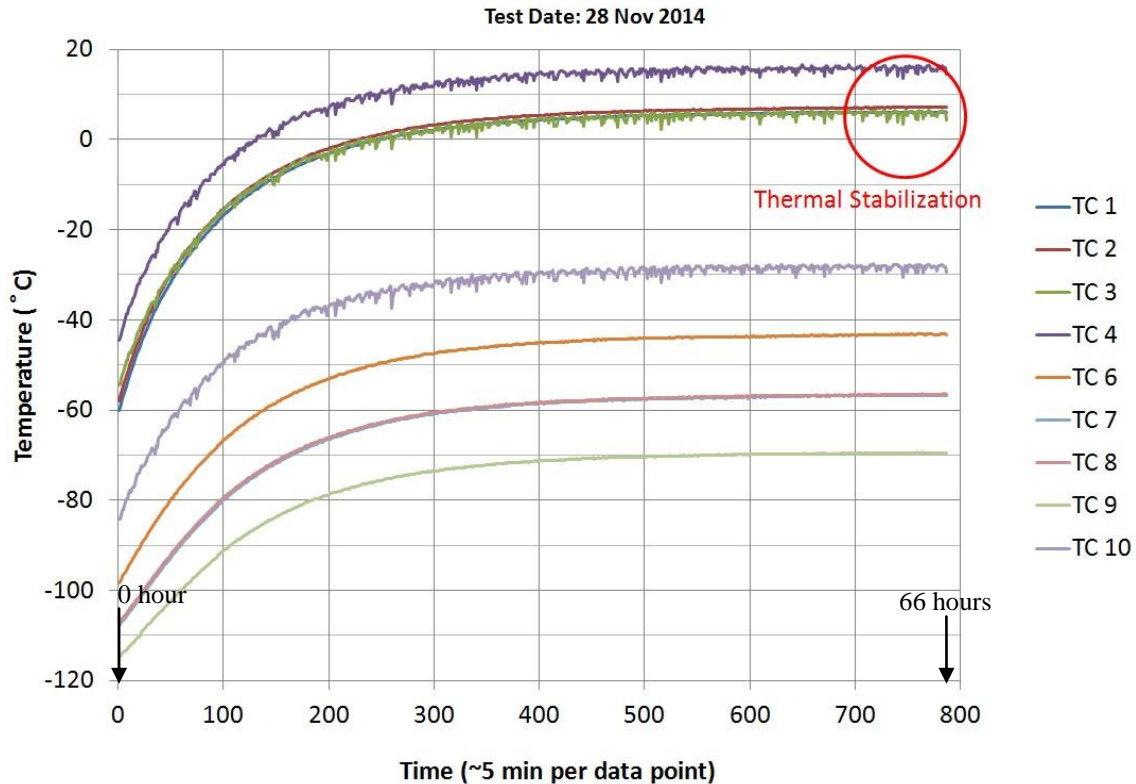
Fig. 23 presents the temperatures of the thermocouples in the cold non-operating thermal balance test with 1.12 W heater power for the EM MAG sensor. The purpose was to determine the sensitivity of the sensor temperature to a reduction in heater power. TC4 was at  $-2^{\circ}\text{C}$ . TC2 and TC3 were at  $-19^{\circ}\text{C}$ . TC1 was at  $-20^{\circ}\text{C}$ . The temperatures of the bobbins are approximately the average ( $-14^{\circ}\text{C}$ ) of TC1, TC2, TC3 and TC4. It agrees with the internal flight telemetry thermistor temperature. It meets the thermal requirement with a smaller margin. A 0.18 W heater power reduction led to a  $15^{\circ}\text{C}$  sensor temperature decrease. Therefore heater power has a large impact on the sensor temperature (approximately  $78^{\circ}\text{C}$  per watt). TC7 and TC8 were at  $-73^{\circ}\text{C}$ . The boom tube temperature was at  $-83^{\circ}\text{C}$ . It shows that as heater power is reduced, the heat leak from the sensor to the boom bracket and boom tube decreases.



**Figure 23. Cold Case Non-Operating Thermal Balance Test Results for 1.12 W Heater Power.**

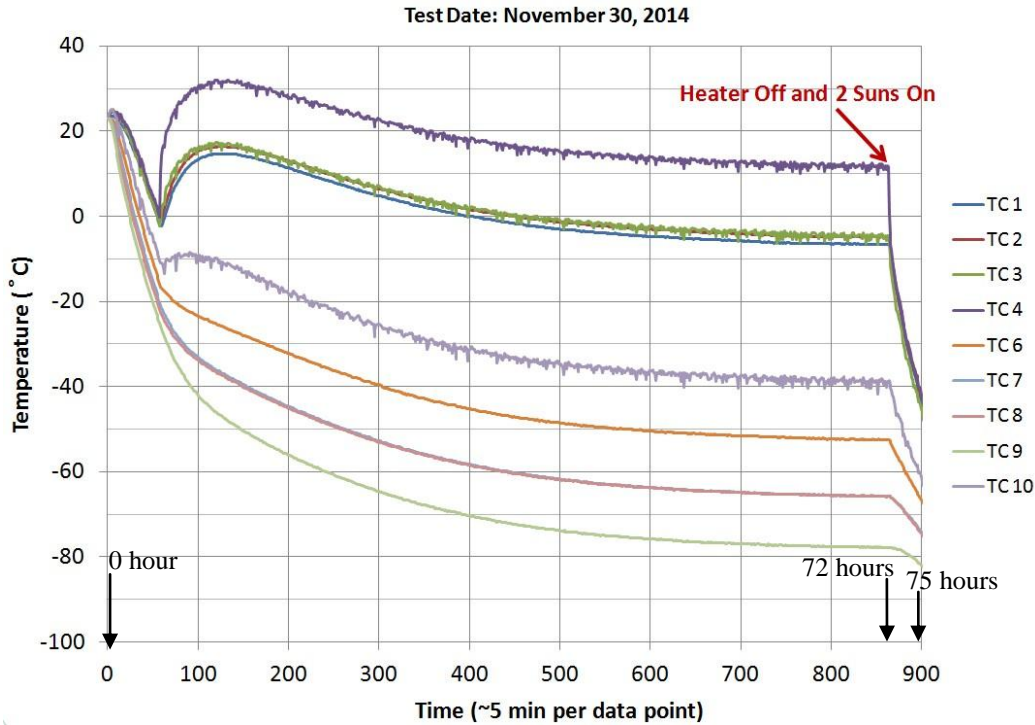
The EM cold case non-operating thermal balance test results show that the temperature gradient between the boom bracket and boom is  $12^{\circ}\text{C}$  for the 1.3 W heater power case, or  $11^{\circ}\text{C}$  for the 1.12 W heater power test case. It verified that the adding thermal isolation between the boom bracket and boom tube reduces the heat leak from the MAG sensor to the boom. As discussed earlier, low emittance tape is also recommended for the boom segment under the boom bracket to minimize heat radiation between the boom bracket and boom tube in flight.

Fig. 24 presents the temperatures of the thermocouples in the hot non-operating thermal balance test with 1.12 W heater power for the EM MAG sensor and simulated solar flux of 2 suns incident on the MAG MLI. The purpose was to determine the sensitivity of the sensor temperature to solar exposure at 0.7 AU. The temperatures of the bobbins are approximately the average ( $9^{\circ}\text{C}$ ) of TC1, TC2, TC3 and TC4. It agrees with the internal flight telemetry thermistor temperature. The results of this test show that solar heating with 2 suns at 0.7 AU increases the MAG sensor bobbin temperature by only about  $23^{\circ}\text{C}$ . This is due to the use of ITO/SiOx/VDA/Kapton as the coating for the sensor MLI outer cover. If StaMet black Kapton were used, the temperature increase will be much larger.



**Figure 24. Hot Case Non-Operating Thermal Balance Test Results for 1.12 W Heater Power and 2 Suns.**

Fig. 25 presents the temperatures of the thermocouples in a 3-hour transient cooldown with no heater power for the EM MAG sensor and simulated solar flux of 2 suns incident on the MAG MLI. With 1.3 W heater power, the sensor temperature was allowed to reach thermal stabilization first (Fig. 22). Then the heater was turned off, and the solar simulator was turned on. The purpose was to determine the thermal capacitance of the sensor. The temperatures of the bobbins at the end of the cooldown are approximately the average ( $-42.2^{\circ}\text{C}$ ) of TC1, TC2, TC3 and TC4. It agrees with the internal flight telemetry thermistor temperature. The results of the transient cooldown test show that without heater power the MAG sensor decreased by about  $47.6^{\circ}\text{C}$  in 3 hours, despite that solar flux of 2 suns was incident on the sensor MLI. It was decreasing at  $17^{\circ}\text{C}$  per hour after 3 hours.



**Figure 25. Transient Cooldown Test Results for No Heater Power and 2 Suns On.**

#### **D. Correlated Thermal Model**

The second EM thermal balance test goal was to correlate the MAG sensor thermal model to the thermal balance test data for use in flight temperature predictions. Based on the flight thermal model, an in-chamber thermal model was developed (Fig. 26).

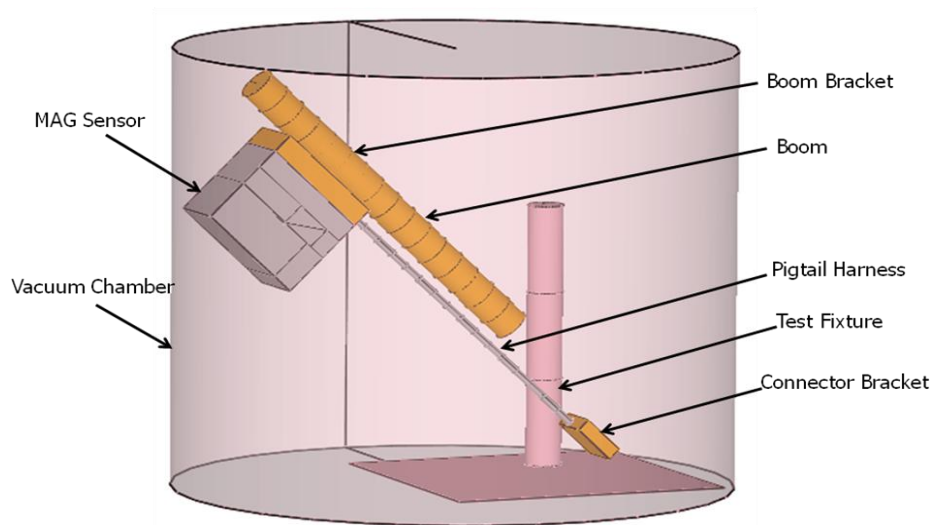


**Figure 26. In-Chamber Thermal Model.**

Correlating the in-chamber thermal model to the thermal balance test results revealed that the MLI  $\epsilon^*$  is 0.075 for the sensor and 0.1 for the pigtail. If the MLI  $\epsilon^*$  values are significantly different from the correlated values, the thermal model won't correlate to within 5°C (maximum allowable at GSFC) of the thermal balance test data. Therefore, these MLI  $\epsilon^*$  values are used in the correlated thermal model for in-flight worst cold case and worst hot case thermal analysis. Removing and re-installing a MLI could change the MLI  $\epsilon^*$  due to workmanship. This was practiced during the one-month long EM sensor thermal balance test. Test results show that it has no observable

effect on the thermocouple temperatures. The MLI  $\epsilon^*$  values of 0.075 for the sensor and 0.1 for the pigtail are expected to be repeatable for the flight MAG sensor MLI. A thermal balance test is planned for the MAG sensor flight unit to re-verify the thermal design, including the MLI  $\epsilon^*$ . Also the Fields instrument level or spacecraft flight system level thermal balance test will re-verify the flight MLI  $\epsilon^*$  at the integrated MAG sensor and boom level.

Correlating the thermal model to the thermal balance test results also revealed the following:

- The total thermal conductance for the kinematic mounts between the sensor base plate and adaptor plate is  $0.0104 \text{ W}^\circ\text{C}^{-1}$ .
- The total thermal conductance for the G-10 spacers and Ti-6Al-4V screws between the adaptor plate and boom bracket is  $0.016 \text{ W}^\circ\text{C}^{-1}$ .
- The thermal conductance between the boom bracket and boom tube is  $0.8 \text{ W}^\circ\text{C}^{-1}$ .
- The thermal conductance between the connector bracket and test fixture is  $0.002 \text{ W}^\circ\text{C}^{-1}$ .
- The MLI  $\epsilon^*$  for the boom and connector bracket MLI is 0.075.
- The total thermal capacitance of the MAG sensor, including the cover, base plate, bobbins, pigtail, adaptor plate and kinematic mounts, is approximately  $264 \text{ J}^\circ\text{g}^{-1}\text{C}^{-1}$ .

Fig. 27 presents the thermal balance test temperature predictions by the correlated thermal model for 1.3 W heater power. Table 3 compares the correlated thermal model temperature predictions to the test data for the four thermal balance test cases. The correlated thermal model predicts temperatures within  $5^\circ\text{C}$  of the test data.

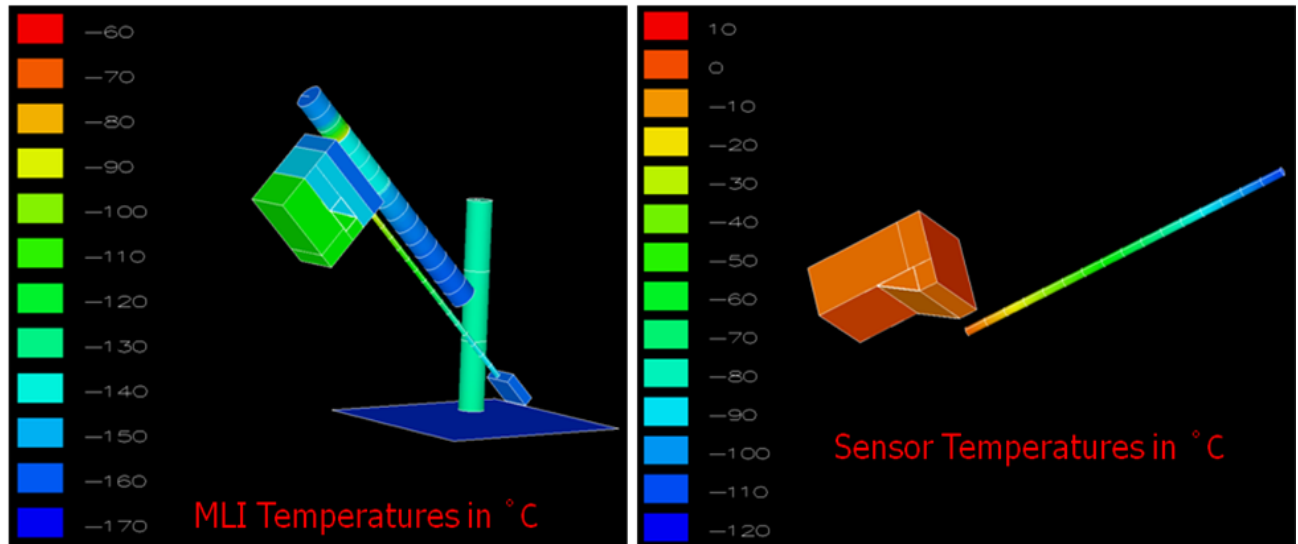


Figure 27. Correlated Thermal Model Predictions for Thermal Balance Test.

Table 3. Comparison of Correlated Thermal Model Predictions and T/B Test Data.

	TC #	1.3 W Heater Power		1.12 Heater Power		1.12 W Heater Power and 2 Suns On		3 Hour Cooldown with Heater Off and 2 Suns On		
		Test Data	Predict	Test Data	Predict	Test Data	Predict	Initial (Test)	Test Data (3 Hr)	Predict (3 Hr)
Sensor Cover	1, 2, 3	-5.4	-1.9	-18.1	-13.7	5.9	7.0	-5.4	-42.2	-38.4
Sensor Adaptor Plate	5, 6	-52.5	-49.0	-58.7	-56.3	-43.3	-45.2	-52.5	-66.0	-63.6
Boom Bracket Interface	7, 8	-65.8	-60.9	-69.7	-67.0	-56.7	-57.6	-65.8	-73.8	-69.7
Boom Adjacent to Boom Bracket	9	-77.8	-77.8	-79.3	-83.1	-69.5	-74.6	-77.8	-81.5	-79.9



### VIII. Flight Temperature Predictions by Correlated Thermal Model

The correlated thermal model is used to predict in-flight worst cold case and worst hot case temperatures for the MAG sensors. Fig. 28 presents the MAG sensor non-operating cold case predictions. Table 4 is a summary of the temperature predictions for selected components. The sensor bobbin and cover temperature predictions are well within the  $-40^{\circ}\text{C}$  to  $60^{\circ}\text{C}$  non-operating AFT limits. As mentioned earlier, due to low power dissipation (0.05 W or less), the sensor operating temperature is no more than  $5^{\circ}\text{C}$  warmer than its non-operating temperature. It will be well within the  $-20^{\circ}\text{C}$  to  $40^{\circ}\text{C}$  operating AFT limits.

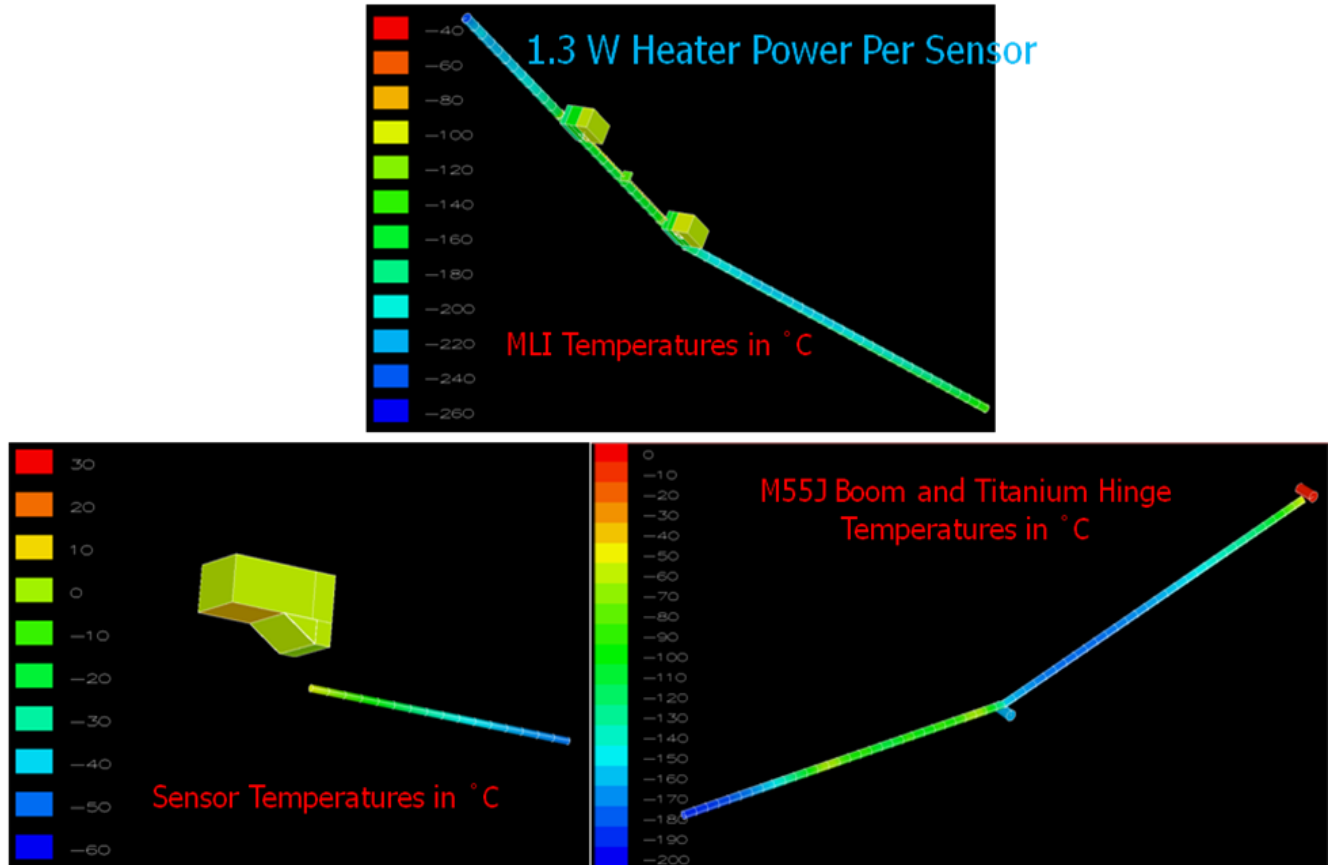


Figure 28. Correlated Thermal Model Predictions for Worst Cold Non-Operating Case Flight Temperatures.

Table 4. Correlated Thermal Model Predictions for Worst Cold Non-Operating Case Flight Temperatures ( $^{\circ}\text{C}$ ).

	Inboard MAG	Outboard MAG
Sensor Cover	4.2	3.6
Sensor Bobbins	6.8	6.1
Sensor Adaptor Plate	-49.4	-49.9
Boom Bracket I/F	-63.9	-63.4
Boom Adjacent to Boom Bracket	-87.2	-86.4

At the CDR, it was necessary to show the MAG thermal detailed design has adequate margins (at least  $5^{\circ}\text{C}$  margin except for heater controlled elements which have a maximum 70% heater duty cycle per GSFC GOLD Rule 4.25). The EM sensor thermal balance test has successfully helped to achieve this goal. Using the correlated thermal model, with 1.3 W heater power the MAG sensor has a maximum heater duty cycle of 67.5% to maintain its operating temperature prediction at  $-20^{\circ}\text{C}$  in the worst cold case when the MAG sensors are in the spacecraft's

umbra. In terms of temperature, the 32.5% (or 0.423 W) heater power margin provides a temperature margin of at least 24 °C for the sensor bobbin and cover. The ratio of delta temperature to delta heater power is 7.3 °C per 100 mW, which is consistent with the EM thermal balance test results which show a 14 °C sensor temperature increase when the heater power was increased from 1.12 W to 1.3 W.

Fig. 29 presents the MAG sensor non-operating worst hot case predictions at 0.7 AU. Table 5 is a summary of the temperature predictions for selected components. A small amount of heater power (0.12 W) maintains the sensor temperature close to that in the worst cold case to minimize the temperature swing during the Comm Slew Downlink. The sensor bobbin and cover temperature predictions have a margin of at least 35 °C when compared to the 60 °C non-operating maximum AFT limit. Therefore the MAG sensor thermal design adequately satisfies GOLD Rule 4.25.

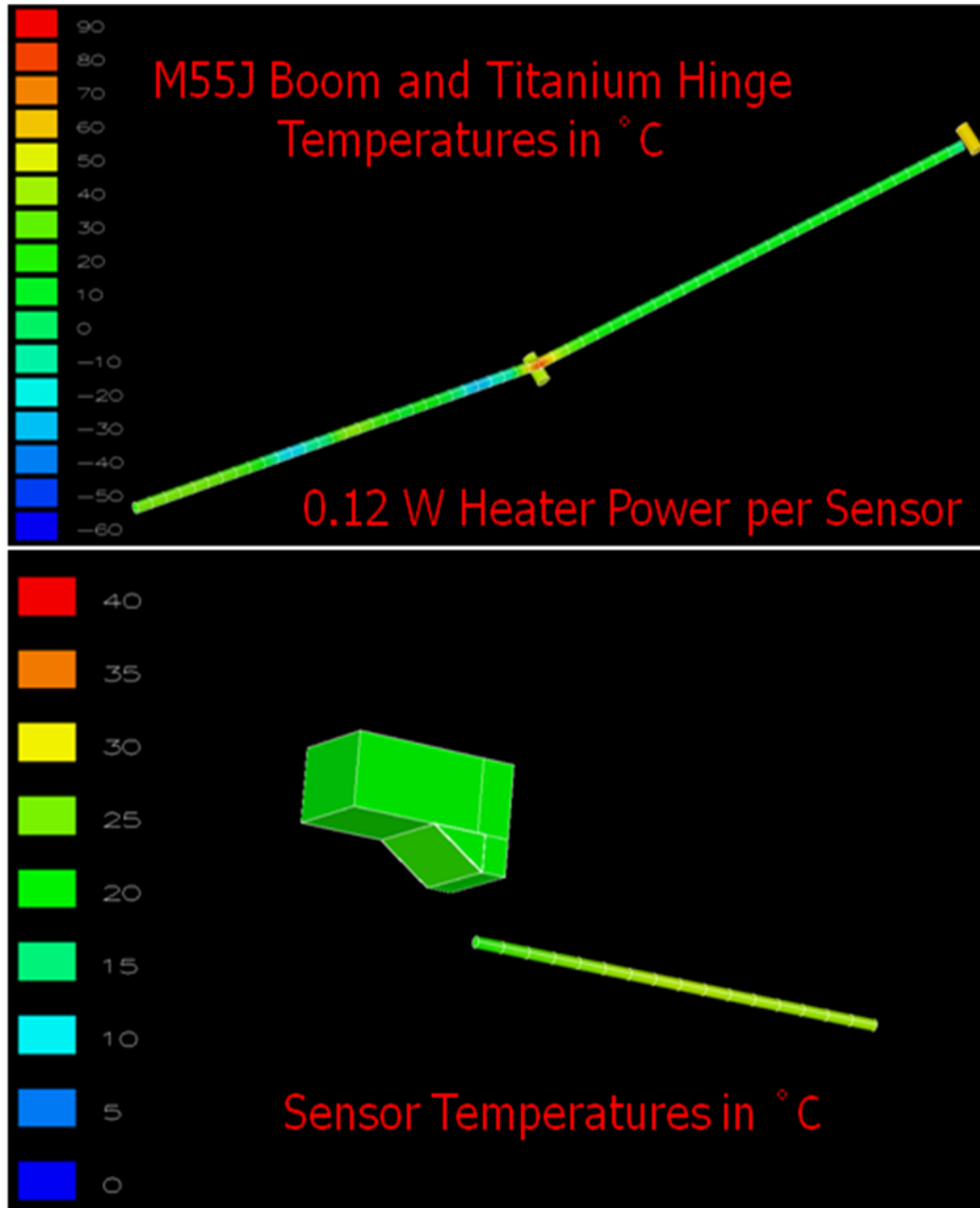


Figure 29. Correlated Thermal Model Predictions for Worst Hot Non-Operating Case Flight Temperatures.

**Table 5. Correlated Thermal Model Predictions for Worst Hot Non-Operating Case Flight Temperatures.**

	Inboard MAG	Outboard MAG
Sensor Cover	14.5	21.4
Sensor Bobbins	19.4	25.3
Sensor Adaptor Plate	-1.8	-0.6
Boom Bracket Interface	-11.8	-4.8
Boom Adjacent to Boom Bracket	-12.2	-5.0

## IX. Conclusion

Thermal design changes have been made to the high-heritage GSFC fluxgate MAG sensor to be flown on SPP. They minimize the conductive heat leak to the boom and radiative heat leak to the space environment. The low heater power budget (about half of the heritage value) and extreme thermal environment drove these design changes. A thermal balance test on the MAG sensor engineering model was completed prior to the FIELDS instrument CDR. It has verified the thermal design and correlated the thermal model. The flight temperature predictions by the correlated thermal model have adequate margins in both the worst hot case and worst cold case.

## References

- <sup>1</sup>Leinweber, H. K., et al., "An Advanced Approach to Finding Magnetometer Zero Levels in the Interplanetary Magnetic Field", *Meas. Sci. Technol.* **19** 055104, 2008.
- <sup>2</sup>Acuna, M., et al., "Space-Based Magnetometers", *Rev. Sci. Instrum.* **73**, 3717 (2002).
- <sup>3</sup>Lepping, R. P., et al., "The Wind Magnetic Field Investigation", *Space Science Reviews*, Volume 71, Issue 1-4, pp. 207-229, 1995.
- <sup>4</sup>Acuna, M., et al., "The STEREO/IMPACT Magnetic Field Experiment", *Space Sci Rev* (2008) 136: 203–226.
- <sup>5</sup>Anderson, B., et al., "The MESSENGER Magnetic Fields Experiment", *Space Sci. Rev.*, 131: 417-540).
- <sup>6</sup>Leidich, J., et al., "Development of a Structural Kinematic Mounting System for Small Payloads", AIAA Paper 2010-6145, 40<sup>th</sup> ICES, Barcelona, Spain, 14 June–2 July, 2010.
- <sup>7</sup>Lin, E. I. et al., "Test-Derived Effective Emittance for Cassini MLI Blankets and Heat Loss Characteristics in the Vicinity of Seams," AIAA Paper 95-2015, June 1995.